

# Charged and Pseudoscalar Higgs production at a Muon Collider

A.G. Akeroyd<sup>a</sup>, A. Arhrib<sup>b,c</sup> and C. Dove

*a: KEK Theory Group, Tsukuba,  
 Ibaraki 305-0801, Japan*

*b: Département de Mathématiques, Faculté des Sciences et Techniques  
 B.P 416, Tanger, Morocco*

*c: UFR-High Energy Physics, Physics Departement, Faculty of Sciences  
 PO Box 1014, Rabat, Morocco*

## Abstract

We consider single charged Higgs ( $H^\pm$ ) and pseudoscalar Higgs ( $A^0$ ) production in association with a gauge boson at  $\mu^+\mu^-$  colliders. We find that the tree-level t-channel and s-channel contributions to  $\mu^+\mu^- \rightarrow H^\pm W^\mp, A^0 Z$  are enhanced for large values of  $\tan\beta$ , allowing sizeable cross-sections whose analogies at  $e^+e^-$  colliders would be very small. These processes provide attractive new ways of producing such particles at  $\mu^+\mu^-$  colliders and are superior to the conventional methods in regions of parameter space.

# 1 Introduction

Charged Higgs bosons ( $H^\pm$ ) are predicted in many favourable extensions of the Standard Model (SM), in particular the Minimal Supersymmetric Standard Model (MSSM). Their phenomenology [1] has received much attention both at  $e^+e^-$  colliders [2] and at hadron colliders [3], [4]. It is well known that  $e^+e^-$  colliders offer a much cleaner environment in which to look than hadron colliders, although recently progress has been made in the possibilities of detecting  $H^\pm$  for  $M_{H^\pm} \geq m_t$  at hadron colliders [5]. At  $e^+e^-$  colliders production proceeds via the mechanism  $e^+e^- \rightarrow \gamma^*, Z^* \rightarrow H^+H^-$ , with higher order corrections evaluated in [6], and detection is possible for  $M_{H^\pm}$  up to approximately  $\sqrt{s}/2$ . The combined null-searches from all four LEP collaborations derive the lower limit  $M_{H^\pm} \geq 77.3$  GeV (95% *c.l.*) [7].

In recent years an increasing amount of work has been dedicated to the physics possibilities of  $\mu^+\mu^-$  colliders [8]. Such colliders offer novel ways of producing Higgs bosons, such as an  $s$ -channel resonance in the case of neutral scalars. The existing studies do not highlight any difference between the charged Higgs phenomenology at a  $\mu^+\mu^-$  collider and  $e^+e^-$  collider, and state that the main production mechanism would be via  $\mu^+\mu^- \rightarrow \gamma^*, Z^* \rightarrow H^+H^-$ . The rate for this process is identical at both colliders. In the MSSM  $H^\pm$  becomes roughly degenerate in mass with  $H^0$  and  $A^0$  for masses greater than 200 GeV. It is this correlation among the masses of the Higgs bosons which disallows any large effects from a  $s$ -channel resonance (via  $\mu^+\mu^- \rightarrow H^0, h^0 \rightarrow H^+H^-$ ) in the pair production mode, and we explicitly confirm this. In order for the above to be maximised one would require  $\sqrt{s} \approx M_{h,H} \geq 2M_{H^\pm}$ , a condition which requires sizeable mass splittings among the Higgs bosons and is disallowed in the MSSM.

So far unconsidered is the process  $\mu^+\mu^- \rightarrow H^\pm W^\mp$  via  $s$ -channel and  $t$ -channel diagrams. Naïvely, this may offer greater possibilities of a large rate since the Yukawa coupling only appears at one vertex in contrast to both vertices in the pair production case. In addition, it offers the possibility of searching for  $M_{H^\pm}$  up to  $\sqrt{s} - M_W$  in contrast to pair production which only probes up to  $M_{H^\pm} \leq \sqrt{s}/2$ . The rate for  $b\bar{b} \rightarrow H^\pm W^\mp$  at hadron colliders was considered in Ref. [9] although is not expected to provide an observable signature above the background [10], at least at LHC energies. In contrast,  $\mu^+\mu^- \rightarrow H^\pm W^\mp$  might give a clean signature, since backgrounds are considerably less.

In an analogous way we also consider  $\mu^+\mu^- \rightarrow A^0 Z$ . The phenomenology of  $A^0$  is made tricky at  $e^+e^-$  colliders due to the absence of a tree-level vertex  $ZZA^0$  and so the standard Higgsstrahlung mechanism ( $e^+e^- \rightarrow A^0 Z$ ) only proceeds via loops [11]. Moreover, over a wide region of parameter space in the MSSM  $A^0$  has a suppressed rate in the channel  $\mu^+\mu^- \rightarrow A^0 h^0$ , while  $\mu^+\mu^- \rightarrow A^0 H^0$  only probes up to  $M_A \approx \sqrt{s}/2$ . Proposed search strategies at  $\mu^+\mu^-$  collider include the scanning technique and Bremsstrahlung tail method. Since both may provide a challenge for machine and detector design we consider the prospects of searching for  $A^0$  via  $\mu^+\mu^- \rightarrow A^0 Z$ .

Our work is organized as follows. In Section 2 we perform the full tree-level calculation of  $\mu^+\mu^- \rightarrow H^+H^-$ ,  $\mu^+\mu^- \rightarrow H^\pm W^\mp$  and  $\mu^+\mu^- \rightarrow A^0 Z$ . In Section 3 we present numerical values of the cross-sections and Section 4 contains our conclusions.

## 2 Calculation

We now consider in turn the various production mechanisms. Our calculations are valid in both the MSSM and a general Two-Higgs-Doublet-Model (2HDM), the difference being that the MSSM Higgs sector is parametrized by just two parameters at tree-level (usually taken as  $M_A$  and  $\tan\beta$ ), while the 2HDM contains 7 free parameters. Thus in a general 2HDM all four Higgs boson masses may be taken as independent, as well as the two mixing angles  $\alpha$  and  $\beta$ , and the Higgs potential parameter  $\lambda_5$  (in the notation of Ref. [12]). In addition, the Higgs trilinear couplings differ from those in the MSSM. In this paper we shall present numerical results for the MSSM. Let us summarise the couplings needed for our study:

### Fermion-Fermion-Higgs couplings

$$\begin{aligned} h^0\mu^+\mu^- &= -\frac{igm_\mu}{2M_W}\lambda_{h\mu^+\mu^-} \quad , \quad H^0\mu^+\mu^- = -\frac{igm_\mu}{2M_W}\lambda_{H\mu^+\mu^-} \\ A^0\mu^+\mu^- &= -\frac{igm_\mu}{2M_W}\gamma_5\lambda_{A^0\mu^+\mu^-} \quad , \quad H^-\mu^+\nu_\mu = \frac{igm_\mu}{\sqrt{2}M_W}\lambda_{H^+\mu^+\nu_\mu}\frac{1-\gamma_5}{2} \end{aligned} \quad (1)$$

In the MSSM these couplings are given by:

$$\begin{aligned} \lambda_{h\mu^+\mu^-} &= -\frac{\sin\alpha}{\cos\beta} \quad , \quad \lambda_{H\mu^+\mu^-} = \frac{\cos\alpha}{\cos\beta} \\ \lambda_{A^0\mu^+\mu^-} &= \tan\beta \quad , \quad \lambda_{H^-\mu^+\nu_\mu} = \tan\beta \end{aligned} \quad (2)$$

One can see from the above formula that the CP-odd  $A^0$  and the charged Higgs bosons coupling to the  $\mu^\pm$  can be enhanced for large  $\tan\beta$ .

The momenta of the incoming  $\mu^+$  and  $\mu^-$ , outgoing gauge boson  $V$  ( $W^\pm$  or  $Z$ ) and outgoing Higgs scalar  $S$  ( $H^\pm$  or  $A^0$ ) are denoted by  $p_{\mu^+}$ ,  $p_{\mu^-}$ ,  $p_V$  and  $p_S$ , respectively. Neglecting the muon mass  $m_\mu$ , the momenta in the centre of mass of the  $\mu^+\mu^-$  system are given by:

$$\begin{aligned} p_{\mu^-, \mu^+} &= \frac{\sqrt{s}}{2}(1, 0, 0, \pm 1) \\ p_{V, A^0} &= \frac{\sqrt{s}}{2}\left(1 \pm \frac{M_V^2 - M_S^2}{s}, \pm \frac{1}{s}\lambda^{\frac{1}{2}}(s, M_V^2, M_S^2)\sin\theta, 0, \pm \frac{1}{s}\lambda^{\frac{1}{2}}(s, M_V^2, M_S^2)\cos\theta\right), \end{aligned}$$

Here  $\lambda(x, y, z) = x^2 + y^2 + z^2 - 2xy - 2xz - 2yz$  is the two body phase space function and  $\theta$  is the scattering angle between  $\mu^+$  and  $S$ ;  $M_V$  is the mass of the gauge boson  $V$  and  $M_S$  is the mass of the Higgs scalar  $S$ . In the case of  $H^+H^-$  production replace  $V$  by  $S$ . The Mandelstam variables are defined as follows:

$$\begin{aligned} s &= (p_{\mu^-} + p_{\mu^+})^2 = (p_V + p_S)^2 \\ t &= (p_{\mu^-} - p_V)^2 = (p_{\mu^+} - p_S)^2 = \frac{1}{2}(M_V^2 + M_S^2) - \frac{s}{2} + \frac{1}{2}\lambda^{\frac{1}{2}}(s, M_V^2, M_S^2)\cos\theta \\ u &= (p_{\mu^-} - p_S)^2 = (p_{\mu^+} - p_V)^2 = \frac{1}{2}(M_V^2 + M_S^2) - \frac{s}{2} - \frac{1}{2}\lambda^{\frac{1}{2}}(s, M_V^2, M_S^2)\cos\theta \\ s + t + u &= M_V^2 + M_S^2 \end{aligned}$$

## 2.1 $\mu^+\mu^- \rightarrow H^+H^-$

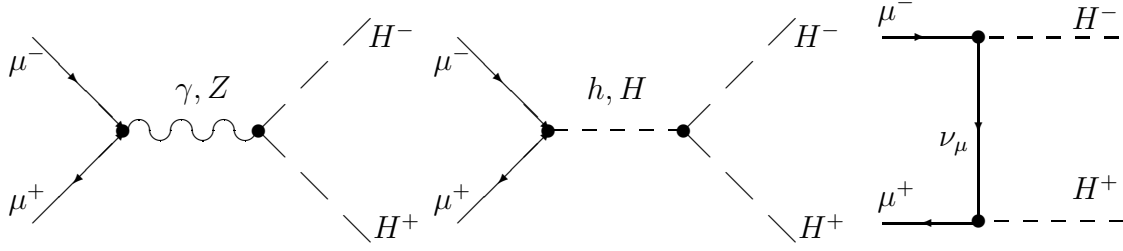


Figure.1

This process proceeds via the conventional Drell–Yan mechanism  $\mu^+\mu^- \rightarrow \gamma^*, Z^* \rightarrow H^+H^-$ , the analogy of  $e^+e^- \rightarrow \gamma^*, Z^* \rightarrow H^+H^-$ . Since  $m_\mu \approx 200m_e$  one may consider the s-channel and t-channel diagrams (see Fig. 1), whose analogies at  $e^+e^-$  colliders would be suppressed by factors of  $m_e$ . The s-channel diagrams would be maximised for  $\sqrt{s} = M_h$  or  $M_H$ , although in the context of the MSSM this condition would not allow on-shell pair production of  $H^\pm$ . This can be seen from the fact that  $\sqrt{s} \geq 2M_{H^\pm}$  and  $\sqrt{s} \approx M_h$  or  $M_H$  cannot be simultaneously satisfied in the MSSM. In contrast, such s-channel diagrams were considered in Ref.[13] for squark production via the process  $\mu^+\mu^- \rightarrow \tilde{q}\tilde{q}$ , and were shown to cause a doubling of the cross-section at resonance. The t-channel diagram in Fig. 1 suffers from Yukawa coupling suppression at two vertices. In the calculation we shall use the following notation:

$$\begin{aligned}
Y_V &= -Y_A = \frac{m_\mu^2}{4s_W^2 M_W^2} \lambda_{H^-\mu\nu_\mu}^2 \\
a_h &= -\frac{g_{hH^+H^-} m_\mu \lambda_{h\mu^+\mu^-}}{2M_W s_W}, \quad a_H = -\frac{g_{HH^+H^-} m_\mu \lambda_{H\mu^+\mu^-}}{2M_W s_W} \\
a_1 &= -2\frac{1}{s} - \frac{1}{2s_W^2 c_W^2} \frac{g_H g_V}{s - M_Z^2 + iM_Z \Gamma_Z} - \frac{Y_V}{t} \\
a_2 &= \frac{1}{2s_W^2 c_W^2} \frac{g_H g_A}{s - M_Z^2 + iM_Z \Gamma_Z} - \frac{Y_A}{t} \\
a_3 &= \frac{a_h}{s - M_h^2 + iM_h \Gamma_h} + \frac{a_H}{s - M_H^2 + iM_H \Gamma_H} + \frac{m_\mu Y_V}{t}
\end{aligned} \tag{3}$$

where  $g_V = -(1 - 4s_W^2)/2$ ,  $g_A = -1/2$  and  $g_H = -c_W^2 + s_W^2$ . The coupling  $g_{hH^+H^-}$  and  $g_{HH^+H^-}$  (normalised to electric charge  $e$ ) are given by:

$$\begin{aligned}
g_{HH^+H^-} &= -\frac{1}{s_W} \left\{ M_W \cos(\beta - \alpha) - \frac{M_Z}{2c_W} \cos 2\beta \cos(\beta + \alpha) + \epsilon \frac{\cos \alpha \cos^2 \beta}{2c_W M_Z \sin \beta} \right\} \\
g_{hH^+H^-} &= -\frac{1}{s_W} \left\{ M_W \sin(\beta - \alpha) + \frac{M_Z}{2c_W} \cos 2\beta \sin(\beta + \alpha) + \epsilon \frac{\sin \alpha \cos^2 \beta}{2c_W M_Z \sin \beta} \right\}
\end{aligned}$$

Where

$$\epsilon = \frac{3G_F m_t^4}{\sqrt{2}\pi^2 \sin^2 \beta} \log \left[ \frac{m_{\tilde{t}_1} m_{\tilde{t}_2}}{m_t^2} \right] \tag{4}$$

The  $\epsilon$  term corresponds to the leading log 1-loop corrections [14] to the trilinear couplings. We will include also these leading log corrections to the Higgs-masses and to the mixing angles.

The square amplitude is given by:

$$|M|^2 = e^4 \left\{ (|a_1|^2 + |a_2|^2) \frac{s^2}{2} \beta_H^2 \sin^2 \theta - 2|a_2|^2 m_\mu^2 s \beta_H^2 + 2|a_3|^2 s + 4\Re(a_1 a_3) m_\mu s \beta_H \cos \theta \right\} \quad (5)$$

with  $\beta_H^2 = 1 - 4M_{H^\pm}^2/s$ . The differential cross-section is given by:

$$\frac{d\sigma}{d\Omega} = \frac{\beta_H}{64\pi^2 s} \frac{1}{4} |M|^2 \quad (6)$$

## 2.2 $\mu^+ \mu^- \rightarrow H^\pm W^\mp$

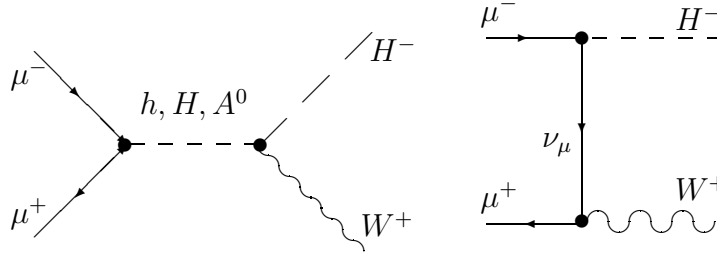


**Figure.2**

Single  $H^\pm$  production may proceed via an s-channel resonance mediated by  $h^0, H^0$  or  $A^0$ , and by t-channel exchange of  $\nu_\mu$  (see Fig. 2). All are negligible at an  $e^+e^-$  collider due to the smallness of  $m_e$ . The loop induced contributions to  $e^+e^- \rightarrow H^\pm W^\mp$  were considered in Ref.[15] and shown to reach a few fb at very low values of  $\tan \beta$ , a region disfavoured in the MSSM. Potential advantages of  $\mu^+ \mu^- \rightarrow H^\pm W^\mp$  over standard pair production are the following:

- $\mu^+ \mu^- \rightarrow H^\pm W^\mp$  is sensitive to the  $H^\pm \mu^\mp \nu_\mu$  Yukawa coupling, which is model dependent, and hence provides information on the underlying Higgs structure. For example, we shall see that a 2HDM with the Model I type structure would not register a signal in this channel. In contrast  $\mu^+ \mu^- \rightarrow \gamma^*, Z^* \rightarrow H^+ H^-$  has a model independent rate.
- Single  $H^\pm$  production is less phase space suppressed than  $H^\pm$  pair production, and would also allow greater kinematical reach at a given collider (on-shell production up to  $\sim \sqrt{s} - M_W$ ).
- The t-channel contribution may be sizeable and does not require  $\sqrt{s} \approx M_{res}$  to be significant, where  $M_{res}$  is the mass of a neutral Higgs s-channel resonance. This is in contrast to other novel production processes at  $\mu^+ \mu^-$  colliders, which usually require the condition  $\sqrt{s} \approx M_{res}$ .

The differential cross-section for  $\sigma(\mu^+\mu^- \rightarrow H^\pm W^\mp)$  may be written as follows:

$$\frac{d\sigma}{d\Omega} = \frac{\lambda^{\frac{1}{2}}(s, M_{H^\pm}^2, M_W^2)}{64\pi^2 s^2} |\mathcal{M}|^2 \quad (7)$$

The matrix element squared is given by:

$$\begin{aligned} |\mathcal{M}|^2 = & \frac{sg^4 m_\mu^2}{32M_W^4} [(|a_V|^2 + |a_A|^2)\lambda(s, M_{H^\pm}^2, M_W^2) + 2a_t^2(2M_W^2 p_T^2 + t^2) \\ & + 2a_t(M_{H^\pm}^2 M_W^2 - sp_T^2 - t^2)\Re(a_V - a_A)] \end{aligned} \quad (8)$$

Where  $p_T^2 = \lambda(s, M_{H^\pm}^2, M_W^2) \sin^2 \theta / 4s$  and the couplings  $a_V, a_A$  and  $a_t$  are given by:

$$a_V = \left( \frac{\cos(\alpha - \beta)\lambda_{h\mu^+\mu^-}}{s - M_h^2 + iM_h\Gamma_h} + \frac{\sin(\alpha - \beta)\lambda_{H\mu^+\mu^-}}{s - M_H^2 + iM_H\Gamma_H} \right) \quad (9)$$

$$a_A = \frac{\lambda_{A\mu^+\mu^-}}{s - M_A^2 + iM_A\Gamma_A} \quad (10)$$

$$a_t = \frac{\lambda_{H^-\mu^+\nu_\mu}}{t} \quad (11)$$

The mixing angle dependence of the Higgs–Fermion–Fermion couplings is contained in  $\lambda_{h\mu^+\mu^-}$ ,  $\lambda_{H\mu^+\mu^-}$ ,  $\lambda_{A\mu^+\mu^-}$  and  $\lambda_{H^-\mu^+\nu_\mu}$ .

Our formula agrees with that for  $b\bar{b} \rightarrow H^\pm W^\mp$  in Ref. [9], with the replacements  $m_t \rightarrow m_{\nu_\mu}$  and  $m_b \rightarrow m_\mu$ . Due to CP-invariance the rate for  $W^+H^-$  and  $W^-H^+$  production is identical.

### 2.3 $\mu^+\mu^- \rightarrow A^0 Z$

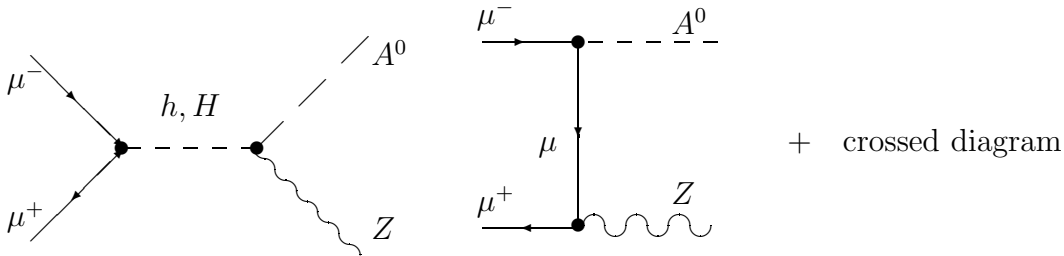


Figure.3

This process proceeds in a very similar way to that for  $\mu^+\mu^- \rightarrow H^\pm W^\mp$ , except there are two t-channel diagrams. This channel would provide an alternative way of searching for  $A^0$  whose detection is not guaranteed at the LHC or a  $\sqrt{s} = 500$  GeV  $e^+e^-$  collider. At the latter this is because the conventional production mechanism  $e^+e^- \rightarrow Z^* \rightarrow A^0 H^0$  would be closed kinematically for  $M_A \approx M_H \geq 250$  GeV, and  $e^+e^- \rightarrow Z^* \rightarrow A^0 h^0$  ( $\sim \cos^2(\beta - \alpha)$ ) is strongly suppressed for  $M_A \geq 200$  GeV. The proposed search at a

$\mu^+\mu^-$  collider for  $M_A \geq \sqrt{s}/2$  is by doing a scan over  $\sqrt{s}$  energies, in order to find a resonance at  $\sqrt{s} = M_A$ , or by running the collider at full  $\sqrt{s}$  and looking for peaks in the  $b\bar{b}$  mass distribution (Bremsstrahlung tail method). These methods are competitive and both may allow detection up to  $M_A \approx \sqrt{s}$  as long as  $\tan\beta \geq 4 - 6$ . However, both may provide quite a demanding challenge for detector resolution and machine design (see Ref. [8]), and it is too early to say with certainty if they would be feasible methods in practice. With this in mind we consider the process  $\mu^+\mu^- \rightarrow A^0 Z$ . With a sizeable rate for  $\sigma(\mu^+\mu^- \rightarrow AZ)$ ,  $A^0$  could be discovered first in this channel, and then the beams could be adjusted to  $\sqrt{s} = M_A$  for precision studies. In addition,  $\mu^+\mu^- \rightarrow A^0 Z$  probes greater masses of  $M_A$  than  $e^+e^- \rightarrow Z^* \rightarrow A^0 H^0$ , and becomes another option to first discover  $A^0$  (if discovery has been elusive at the LHC or a  $\sqrt{s} = 500$  GeV  $e^+e^-$  collider). The matrix element squared may be written as:

$$\begin{aligned}
|\mathcal{M}|^2 = & \frac{sg^4 m_\mu^2}{32M_W^4} [|a_V|^2 \lambda(s, M_A^2, M_Z^2) - 2a_{t1}g_A(M_A^2 M_Z^2 - sp_T^2 - t^2) \Re(a_V) \\
& - 2a_{t2}g_A(M_A^2 M_Z^2 - sp_T^2 - u^2) \Re(a_V) \\
& + (g_A^2 + g_V^2) \{a_{t1}^2(2M_Z^2 p_T^2 + t^2) + a_{t2}^2(2M_Z^2 p_T^2 + u^2)\} \\
& - 2(g_A^2 - g_V^2)a_{t1}a_{t2}(2M_Z^2 p_T^2 + 2M_A^2 M_Z^2 - tu)]
\end{aligned} \tag{12}$$

with  $a_V$  the same as in Section 2.2 and

$$a_{t1} = \frac{\lambda_{A\mu^+\mu^-}}{t - m_\mu^2}, \quad a_{t2} = \frac{\lambda_{A\mu^+\mu^-}}{u - m_\mu^2} \tag{13}$$

The differential cross-section follows from eq(7) with the changes  $M_{H^\pm} \rightarrow M_A$  and  $M_W \rightarrow M_Z$ .

### 3 Numerical results

We now present our numerical analysis in the context of the MSSM. We take  $\sqrt{s} = 500$  GeV and assume integrated luminosities of the order  $50 \text{ fb}^{-1}$ .

In Fig. 4 we plot  $\sigma(\mu^+\mu^- \rightarrow H^\pm W^\mp)$ , defined as the sum of  $H^+W^-$  and  $H^-W^+$  production, as a function of  $M_{H^\pm}$ , varying  $\tan\beta$  from 20 to 50. We also include the tree-level rate for  $\sigma(e^+e^- \rightarrow H^+H^-)$  in order to show the advantage of a  $\mu^+\mu^-$  collider over an  $e^+e^-$  collider. One can see that the single production mode gains in importance with increasing  $\tan\beta$ , and offers detection possibilities for  $M_{H^\pm}$  up to  $\sqrt{s} - M_W$ . This compares favourably with the reach at an  $e^+e^-$  collider.

The slight dip and rise of the curves arises due to the  $H^0$  and  $A^0$  mediated s-channel contributions increasing in magnitude with  $M_{H^\pm}$ , which compensates for the phase space suppression until the kinematical limit is approached. This can be seen from the fact that since  $M_{H^\pm} \approx M_H \approx M_A$ , larger  $M_{H^\pm}$  causes both  $M_H$  and  $M_A$  to be closer to  $\sqrt{s}$  (i.e. the resonance condition).

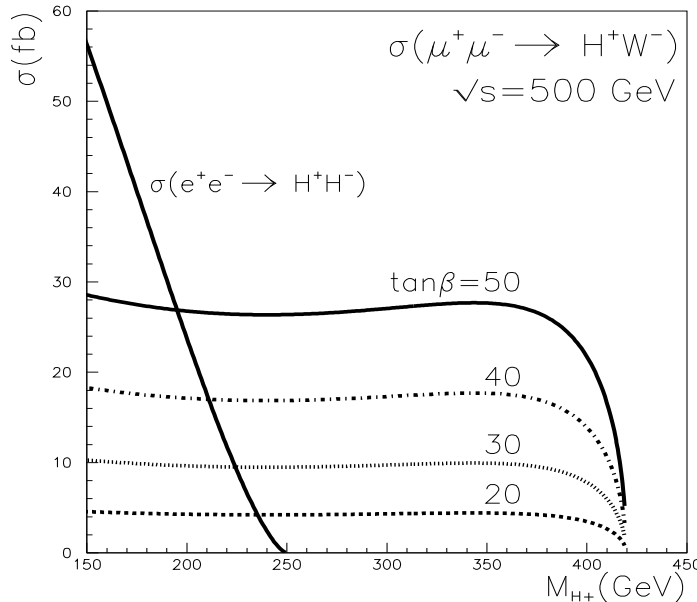


Figure 4:  $\sigma(\mu^+\mu^- \rightarrow H^\pm W^\mp)$  as a function of  $M_{H^\pm}$  for various values of  $\tan\beta$ . Also indicated is  $\sigma(e^+e^- \rightarrow H^+H^-)$  for the same  $\sqrt{s}$ .

It is clear from the graphs that for  $\tan\beta \geq 20$  one has  $\sigma(\mu^+\mu^- \rightarrow H^\pm W^\mp) \geq 5$  fb, which would give a sizeable number of singly produced  $H^\pm$  for luminosities of  $50 \text{ fb}^{-1}$ . One would expect  $H^\pm \rightarrow tb$  decays for the mass region of interest and so the main background would be from  $t\bar{t}$  production. Such a background [10] was shown to overwhelm the channel  $pp \rightarrow H^\pm W^\mp$  [9] at the LHC. However, at a  $\sqrt{s} = 500$  GeV muon collider  $\sigma(\mu^+\mu^- \rightarrow t\bar{t}) \sim 0.7$  pb in contrast to  $\sim 800$  pb at the LHC. Hence we would expect much better prospects for detection at a muon collider although a full signal-background analysis is beyond the scope of this paper. Previous studies of backgrounds to  $H^\pm W^\mp$  production at  $e^+e^-$  colliders have been carried out in the context of Higgs triplet models [16], assuming  $H^\pm \rightarrow W^\pm Z$  as the main decay channel. Such studies cannot be applied to the MSSM where  $H^\pm \rightarrow tb$  decays would dominate.

We note that a 2HDM with the Model I type structure would not register an observable signal in this channel. This is due to the rate being proportional to  $\cot^2\beta$ , and so unacceptably small values of  $\tan\beta$  would be required in order to allow observable cross-sections.

The process  $\mu^+\mu^- \rightarrow A^0 Z$  suffers from smaller cross-sections and these are plotted as a function of  $M_A$  in Fig. 5. Given that  $\mu^+\mu^- \rightarrow A^0 H^0$  probes  $M_A$  up to  $\approx \sqrt{s}/2$  the region  $M_A \geq 250$  GeV is of interest. We see that cross-sections  $\geq 1$  fb are only attainable in this region for  $\tan\beta \geq 30$  and so detection would be restricted to large values of  $\tan\beta$ .



The smallness of the cross-sections is caused by large destructive interference between the  $s$  and  $t$  channels.

Finally, we consider  $\mu^+\mu^- \rightarrow H^+H^-$ . We find very small deviations from the rate for  $e^+e^- \rightarrow H^+H^-$ , of the order a few percent for large values of  $\tan\beta$ . This can be traced to the fact that the  $s$ -channel Higgs exchange diagrams are far from resonance, and the  $t$ -channel diagrams are doubly Yukawa suppressed. Since the 1-loop corrections [6] may be much larger than these deviations we do not plot a graph.

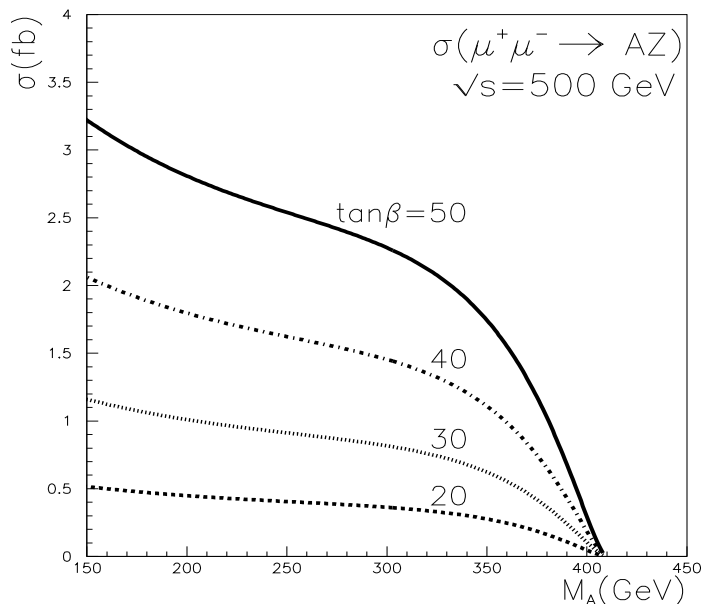


Figure 5:  $\sigma(\mu^+\mu^- \rightarrow A^0Z)$  as a function of  $M_A$  for various values of  $\tan\beta$ .

## 4 Conclusions

We have considered the processes  $\mu^+\mu^- \rightarrow H^\pm W^\mp$  and  $\mu^+\mu^- \rightarrow A^0Z$  of the MSSM in the context of a high-energy  $\mu^+\mu^-$  collider ( $\sqrt{s} = 500$  GeV). We showed that  $\mu^+\mu^- \rightarrow H^\pm W^\mp$  production offers an attractive new way of searching for  $H^\pm$  at such colliders. The cross-section grows with increasing  $\tan\beta$  with values as large as 30 fb being attainable for  $\tan\beta \geq 50$ . With an integrated luminosity of  $50 \text{ fb}^{-1}$  a significant number of  $H^\pm$  could be produced singly up to  $M_{H^\pm} \approx \sqrt{s} - M_W$ . This compares favourably with the reach at an  $e^+e^-$  collider, which may only probe up to  $M_{H^\pm} \approx \sqrt{s}/2$ . The main background (assuming  $H^\pm \rightarrow tb$  decays) would be from  $t\bar{t}$  production, which has a cross-section of 700 fb, 3 orders of magnitude less than at the LHC. We conclude that the mechanism

$\mu^+\mu^- \rightarrow H^\pm W^\mp$  represents a novel and attractive way of producing  $H^\pm$  at a  $\mu^+\mu^-$  collider, and in our opinion merits a detailed signal-background analysis.

Pseudoscalar Higgs production via  $\mu^+\mu^- \rightarrow A^0 Z$  offers smaller cross-sections, with values of 2 fb or more only possible for large ( $\geq 40$ )  $\tan\beta$ . Charged Higgs pair production has essentially the same rate as that at an  $e^+e^-$  collider, with differences of the order of a few percent for large values of  $\tan\beta$ .

## Acknowledgements

A.G. Akeroyd was supported by the Japan Society for Promotion of Science (JSPS). We thank A. Turcot for useful comments.

## References

- [1] J.F. Gunion, H.E. Haber, G.L. Kane and S. Dawson, *The Higgs Hunter's Guide* (Addison-Wesley, Reading, 1990).
- [2] S. Komamiya, Phys. Rev. **D38** (1988) 2158; A. Sopczak, Z.Phys. **C65** (1995) 449; S. Moretti and K. Odagiri, J. Phys. **G23** (1997) 537.
- [3] E. Eichten, I. Hinchliffe, K. Lane and C. Quigg, Rev. Mod. Phys. **56** (1984) 579; J. Gunion, H.E. Haber, F.E. Paige, W.K. Tung and S.S.D. Willenbrock, Nucl. Phys. **B294** (1987) 621; R.M. Barnett, H.E. Haber and D.E. Soper, **B306** (1988) 697; D.A. Dicus, J.L. Hewett, C. Kao, and T.G. Rizzo, Phys. Rev. **D40** (1989) 787; V. Barger, R.J.N. Philips and D.P. Roy, Phys. Lett. **B324** (1994) 236; J.L. Diaz-Cruz and O.A. Sampayo, Phys. Rev. **D50** (1994) 6828.
- [4] Jiang Yi, Ma Wen-Gan, Han Liang, Han Meng and Yu Zeng-hui; J. Phys. **G24** (1998) 83; J. Phys. **G23** (1997) 385; A. Krause, T. Plehn, M. Spira and P.W. Zerwas, Nucl. Phys. **B519** (1998) 85; S. Moretti and K. Odagiri, Phys. Rev. **D55** (1997) 5627; Li Gang Jin, Chong Sheng Li, R.J. Oakes and Shou Hua Zhu, hep-ph/9907482; A.A. Barrientos Bendezu and B.A. Kniehl, hep-ph/9908385.
- [5] K. Odagiri, Phys. Lett. **B452** (1999) 327; K. Odagiri, hep-ph/9901432; D.P. Roy, hep-ph/9905542; D.J. Miller, S. Moretti, D.P. Roy and W.J. Stirling, hep-ph/9906230.
- [6] A. Arhrib, M. Capdequi Peyranère and G. Moultaka, Phys. Lett. **B341** (1995) 313; M.A. Diaz and Tonnis A. ter Veldhuis, hep-ph/9501315; A. Arhrib and G. Moultaka, hep-ph/9808317, to appear in Nucl. Phys. B.
- [7] Combined Experimental Limits; ALEPH 99-081 CONF 99-052; DELPHI 99-142 CONF 327; L3 Note 2442; OPAL Technical Note TN-614.

- [8] *Proceedings of the Workshop on Physics at the First Muon Collider and front end of a Muon Collider*, Fermilab, November 6-9, 1997;  *$\mu^+\mu^-$  Collider: a Feasibility Study*, BNL-52503, Fermilab-Conf-96/092, LBNL-38946, July 1996; Phys. Rep. 286 (1996) 1.
- [9] A.A. Barrientos Bendezu and B.A. Kniehl, Phys. Rev. **D59** (1999) 015009.
- [10] S. Moretti and K. Odagiri, Phys. Rev. **D59** (1999) 055008.
- [11] A.G. Akeroyd, A. Arhrib and M. Capdequi Peyranère, hep-ph/9907542 (Mod. Phys. Lett. A, in press)
- [12] A. Djouadi, V. Driesen, W. Hollik and A. Kraft, Eur. Phys. J. **C1** (1998) 163.
- [13] A. Bartl, H. Eberl, K. Hidaka, S. Kraml, W. Majerotto, W. Porod and Y. Yamada, Phys. Rev. **D58** (1999) 115002.
- [14] Y. Okada, M. Yamaguchi and T. Yanagida, Prog. Theo. Phys. **85** (1991) 1; H. Haber and R. Hemping, Phys. Rev. Lett. **66** (1991) 1815; J. Ellis, G. Ridolfi and F. Zwirner, Phys. Lett. **B257** (1991) 83; R. Barbieri, F. Caravaglios and M. Frigeni, Phys. Lett. **B258** (1991) 167.
- [15] Shou Hua Zhou, hep-ph/9901221.
- [16] K. Cheung, R.J.N. Phillips and A. Pilaftsis, Phys. Rev. **D51** (1995) 4731; D.K. Ghosh, R.M. Godbole and B. Mukhopadhyaya, Phys. Rev. **D55** (1997) 3150.